

ORIGINAL PAPERS

BCL-x_L and BCL2 delay Myc-induced cell cycle entry through elevation of p27 and inhibition of G1 cyclin-dependent kinases

Courtney Greider², Anuja Chattopadhyay¹, Christina Parkhurst¹ and Elizabeth Yang^{*1,2}

¹Department of Pediatrics, Vanderbilt-Ingram Cancer Center, Vanderbilt University School of Medicine, Nashville, Tennessee, TN 37232, USA; ²Department of Cancer Biology, Vanderbilt-Ingram Cancer Center, Vanderbilt University School of Medicine, Nashville, Tennessee, TN 37232, USA

The anti-apoptotic molecules BCL-x_L and BCL2 delay cell cycle entry from quiescence. We used serum induction and induction of a Myc-estrogen receptor fusion protein (MycER) in quiescent fibroblasts to investigate the mechanisms underlying the cell cycle activity of BCL-x_L and BCL2. We demonstrate for the first time that BCL-x_L and BCL2 delayed serum-induced and Myc-induced, but not E2F-induced, cell cycle entry. The cyclin-dependent kinase inhibitor p27 was elevated during serum deprivation and cell cycle entry in BCL-x_L or BCL2-expressing NIH3T3 cells and a Rat1MycER cell line. Activation of cyclin-dependent kinase 2 (cdk2) and cyclin-dependent kinase 4 (cdk4) were delayed during progression to S phase, while the induction of cyclin D1 protein, as well as the levels of cyclin E, cdk2, and cdk4 were unaltered by BCL-x_L or BCL2. Inhibition of cyclin/cdk activities in BCL-x_L or BCL2 expressing cells was associated with excess p27 in the cyclin/cdk complexes. Neither BCL-x_L nor BCL2 delayed S phase entry in cells deficient in p27, thus p27 is required for the cell cycle function of BCL-x_L and BCL2. The cell cycle effects of BCL-x_L and BCL2 were more profound in Myc-induced than in serum-induced cell cycle entry. Our results suggest that one possible mechanism by which BCL-x_L and BCL2 delay cell cycle entry may be the inhibition of Myc activity through the elevation of p27.

Oncogene (2002) 21, 7765–7775. doi:10.1038/sj.onc.1205928

Keywords: BCL2; BCL-x_L; cell cycle; p27; cdk; Myc

Introduction

The anti- and pro-apoptosis functions of the BCL2 family of molecules have been extensively investigated. However, selected members of the BCL2 family also have cell cycle effects. The ability of BCL2 and BCL-x_L to delay cell cycle progression is most obvious during entry into S phase from quiescence. In transgenic BCL2 mouse models, S phase entry after T cell activation is

retarded, while *bcl2*^{-/-} T cells exhibit accelerated activation-induced cell cycle entry (Linette *et al.*, 1996; Mazel *et al.*, 1996). In cultured fibroblasts, BCL2 and BCL-x_L delay serum-induced cell cycle entry (O'Reilly *et al.*, 1996; Huang *et al.*, 1997). Conversely, T cells bearing the pro-apoptotic BAX transgene demonstrate faster T-cell activation induced cell cycle entry (Brady *et al.*, 1996). BAD, which contains only one of the BCL2-homology domains BH3, heterodimerizes with BCL2 and BCL-x_L and impairs the ability of cells to effectively arrest in G0/G1 (Chattopadhyay *et al.*, 2001). The classic model of BCL2-mediated oncogenesis states that BCL2 inhibits cell death without affecting proliferation (Hueber and Evan, 1998). Yet cells protected from apoptosis by BCL2 are often quiescent, while the execution of cell death is frequently associated with cycling cells, suggesting that the cell cycle delay effect of BCL2 and BCL-x_L could be linked to their anti-apoptosis function. While BCL2 and BCL-x_L do not noticeably affect cell cycle progression of proliferating cells, their ability to retain cells in quiescence may contribute to oncogenicity.

BCL2 acts in G0 and at the G1/S transition. BCL2 can hasten exit to G0 (Vairo *et al.*, 1996), and cells expressing BCL2 achieve a very efficient G0 arrest. In IL-3-dependent hematopoietic cells and fibroblasts which are arrested in G0 and stimulated to re-enter the cell cycle by IL-3 or by the addition of serum, BCL2 lengthens the time to reach S phase (Huang *et al.*, 1997). Investigations into the mechanism of the delayed G1/S transition have focused on p27 and the Rb/E2F complex. In multiple cell types expressing BCL2, p27 protein is increased and Rb is more hypophosphorylated (Brady *et al.*, 1996; Linette *et al.*, 1996; Vairo *et al.*, 2000). Phosphorylation of Rb releases free E2F, which is transcriptionally active and promotes entry into S phase. BCL2 has been shown to function through the pRB family member p130 in a complex with E2F4 to negatively regulate E2F1, thus inhibiting cell cycle progression (Lind *et al.*, 1999; Vairo *et al.*, 2000).

Progression from G0/G1 to S is orchestrated by a sequence of events including induction of early genes such as Myc, Jun, Fos, loss of cdk (cyclin-dependent kinase) inhibitors, induction of cyclin D and cyclin E, and activation of cdk4 and cdk2, resulting in phosphorylation of pRB and activation of E2F. The cdk inhibitors consist of the Cip/Kip proteins, including p27, p21, and p57, which can inhibit all cyclin/cdks, and the INK4 family

*Correspondence: E Yang, 397 PRB, Vanderbilt Medical Center, Nashville, Tennessee, TN 37232, USA;
E-mail: elizabeth.yang@vanderbilt.edu
Received 17 July 2002; revised 24 July 2002; accepted 1 August 2002

such as p16 and p15, which selectively inhibit cdk4 and cdk6 complexes. p27 is a prominent negative regulator of cell cycle in fibroblasts and many other cell types. It is abundant in quiescent cells, binds and inhibits cyclin E/cdk2, and rapidly decreases as cells traverse G1 to reach S phase. Regulation of p27 is largely posttranslational (Philipp-Staheli *et al.*, 2001). Phosphorylation targets p27 for degradation by the ubiquitination/proteasome pathway, and G1 progression causes p27 to be sequestered away from cyclin E/cdk2 by proteins such as cyclin D1 and D2 (Bouchard *et al.*, 1999; Perez-Roger *et al.*, 1997, 1999). p27 can also be transcriptionally regulated by Myc (Yang *et al.*, 2001) and forkhead transcription factors (Dijkers *et al.*, 2000; Medema *et al.*, 2000). In addition, subcellular localization plays a major role in p27 regulation. p27 needs to be imported into the nucleus to function in G1 and its degradation is linked to nuclear export (Tomoda *et al.*, 1999, 2001).

Myc is induced early in cell cycle entry, and activation of cyclin E/cdk2 is critical for Myc-induced cell cycle progression (Obaya *et al.*, 1999). Myc can regulate p27 by multiple mechanisms. These include disruption of p27 binding to cyclin E/cdk2 (Perez-Roger *et al.*, 1999; Bouchard *et al.*, 1999), promotion of p27 degradation (O'Hagan *et al.*, 2000), and transcriptional repression (Obaya *et al.*, 1999; Yang *et al.*, 2001). In the absence of serum, induction of Myc alone is sufficient to induce cell cycle entry and cell death; thus, Myc causes both proliferation and apoptosis (Eilers *et al.*, 1991; Evan *et al.*, 1992). The observation that BCL2 cooperates with Myc in oncogenesis has been explained by the ability of BCL2 to counter Myc-induced apoptosis without altering the proliferative effect of Myc (Fanidi *et al.*, 1992; Marin *et al.*, 1995; Cory *et al.*, 1999; Hueber and Evan, 1998).

A classical system for studying cell death and cell cycle uses the inducible MycER fusion protein (Obaya *et al.*, 1999). Inhibition of MycER-induced apoptosis by BCL2 is well studied (Evan *et al.*, 1992), but the effect of BCL2 on MycER-induced S phase progression has not been mechanistically examined. We used Rat1 cells expressing MycER (Rat1/MycER) and NIH3T3 fibroblasts to ask which of the known cell cycle events is altered by BCL2 or BCL-x_L. BCL2 and BCL-x_L inhibited Myc-induced cell cycle entry. BCL2 and BCL-x_L significantly delayed activation of cyclin/cdk activities, in both serum-induced and Myc-induced cell cycle entry, without affecting cyclin induction. Rather, the cdk inhibitor p27 was elevated in cells expressing BCL2 or BCL-x_L, and Myc-induced dissociation of p27 from cyclin E/cdk2 was impaired in BCL-x_L expressing cells. Finally, the cell cycle delay activity of BCL-x_L and BCL2 required the presence of p27.

Results

BCL-x_L and BCL2 delay serum-induced and Myc-induced, but not E2F-induced, cell cycle entry

NIH3T3 cells expressing BCL2, BCL-x_L, or vector alone were arrested in G0/G1 by serum starvation and

induced to re-enter the cell cycle by serum stimulation. S phase entry, as measured by propidium iodide staining of DNA content (Figure 1A) and BrdU incorporation (data not shown), was delayed by 4 h in BCL2 or BCL-x_L expressing cells, consistent with previous reports (O'Reilly *et al.*, 1996). To begin probing the mechanism of cell cycle delay by BCL-x_L and BCL2, we asked whether the activity of BCL-x_L or BCL2 can be temporally placed in the sequence of events occurring between G0/G1 and G1/S. Myc induction is an early event in G1 progression, and ectopic expression of Myc in the absence of serum is sufficient to drive entry into S phase (Kaczmarek *et al.*, 1985; Eilers *et al.*, 1991). To assess whether BCL-x_L or BCL2 can delay Myc-induced cell cycle entry, BCL-x_L and BCL2 were expressed in Rat1MycER cells by retroviral infection, and puromycin resistant cells were analysed as pools. Rat1MycER cells expressing BCL-x_L, BCL2, or vector alone were serum starved for 48 h, then treated with 4-hydroxy-tamoxifen (4-OHT) to activate Myc without addition of serum. The rate of cell cycle entry induced by Myc was assessed by propidium iodide (PI)/FACS analysis and BrdU analysis (Figure 1B). PI analysis showed that, compared to asynchronous cultures in 10% serum where 35–40% of the cells were in S phase, MycER cells cultured in 0.05% serum for 48 h exhibited significantly less S phase cells (14%), but were not fully arrested. After Myc induction by 4-OHT, vector alone control cells progressed into S phase as early as 3–4 h. MycER cells expressing either BCL-x_L or BCL2 were virtually all arrested in G0/G1 after 48 h of serum starvation. These cells only began to enter S phase 12 h after the addition of 4-OHT, and did not exhibit significant S phase cells until 16 h after Myc induction. The inability of MycER/pBabe cells to fully arrest after serum starvation is most likely due to leakiness of the MycER system. To be certain that the increase in cells with S phase DNA content was due to cell cycle progression and not a relative loss of G1 or G2/M cells due to apoptosis, BrdU pulse-labeling was performed during 4-OHT treatment. These results confirmed that BCL-x_L (Figure 1B) and BCL2 (data not shown) expression delayed Myc-induced S phase entry. Thus, BCL-x_L or BCL2 expression delayed Myc-induced cell cycle entry by 8–9 h. Myc-induced apoptosis was completely inhibited by BCL-x_L or BCL2 (Figure 1B), as expected.

Similar to the induction of Myc, activation of E2F in the absence of serum also induces cell cycle progression (Shan and Lee, 1994; Johnson *et al.*, 1993) and causes apoptosis (Wu and Levine, 1994). E2F transcriptionally activates target genes at the G1/S boundary when it is released from Rb; therefore, E2F activation is a late event in S phase entry. To determine whether BCL-x_L and BCL2 can delay E2F-induced cell cycle progression, BCL-x_L and BCL2 were introduced by retroviral infection into Rat2 cells harboring tetracycline-repressible E2F-1 (FBX40) (Shan and Lee, 1994). Vector alone control FBX40 and BCL-x_L- or BCL2-expressing FBX40 cells were cultured in 0.05% serum

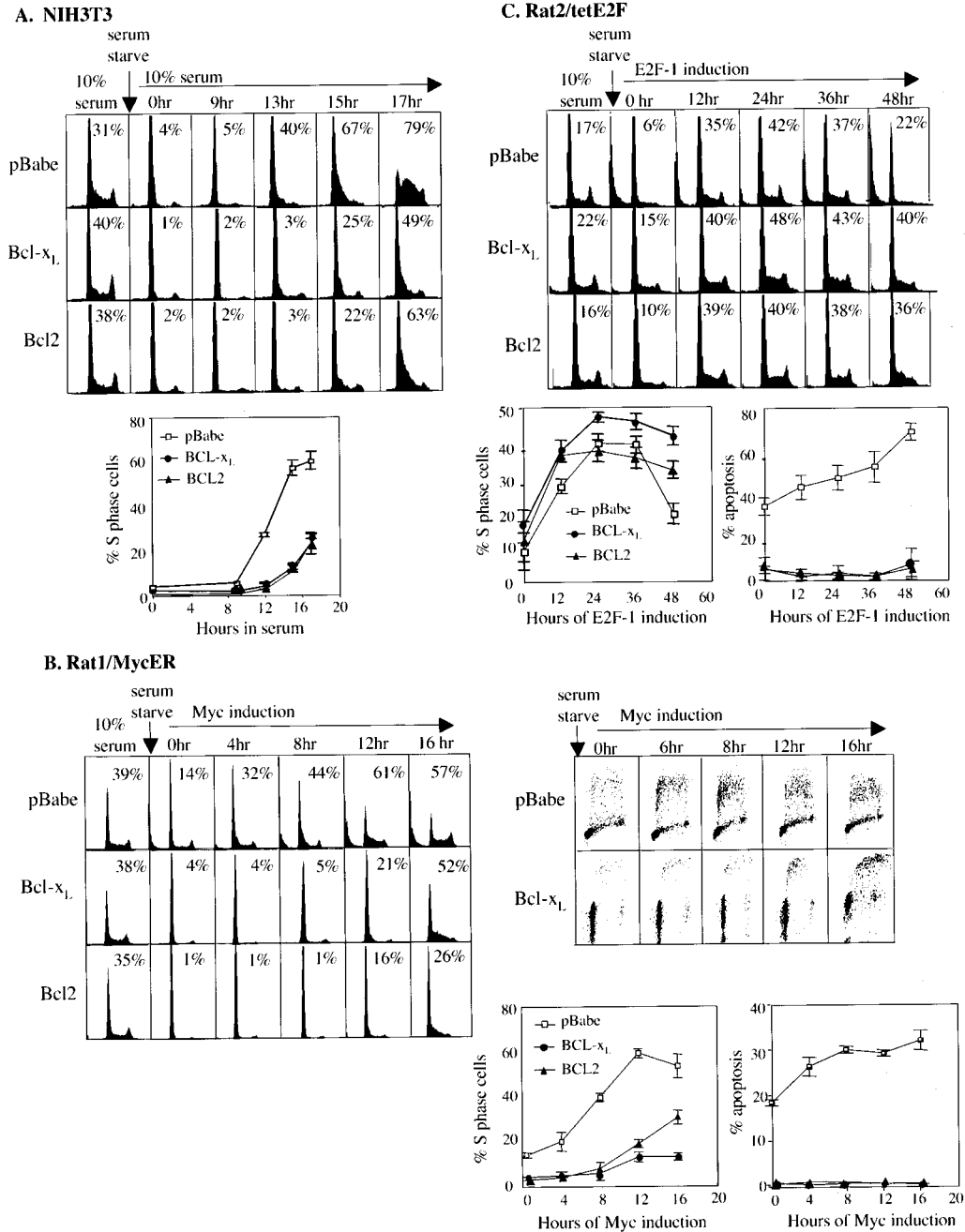


Figure 1 BCL-x_L and BCL2 delay S phase entry stimulated by serum and Myc induction, but not E2F induction. (A) NIH3T3 cells were cultured in 0.75% BS for 48 h and stimulated to re-enter the cell cycle with 10% BS. (B) Rat1MycER cells were cultured in 0.05% FBS for 48 h and stimulated with 200 nM 4-OHT. (C) Rat2/tetE2F (FBX40) cells were cultured in 0.05% FBS containing tetracycline for 48 h and stimulated by changing the media to 0.05% FBS without tetracycline. DNA content at indicated time-points were obtained by PI staining and FACS analysis. Percentages of S phase cells are shown for each cell cycle profile and are also shown graphically. Error bars are derived from five experiments for NIH3T3 cells, four experiments for Rat1/MycER cells, and four experiments for Rat2/tetE2F cells. For some time points, the standard deviations are so tight such that error bars are not visible. Open square, vector alone control cells; closed circle, BCL-x_L expressing cells; closed triangle, BCL2 expressing cells. BrdU incorporation versus PI staining plots are shown for MycER/pBabe and MycER/Bcl-x_L cells. Cells containing <2N DNA were represented as percentage of apoptosis in B and C

with tetracycline for 48 h, then switched to 0.05% serum without tetracycline and followed for cell cycle progression (Figure 1C). All cultures showed significant increases in S phase cells by 12 h after E2F induction.

At later time points, BCL-x_L and BCL2 expressing FBX40 cultures had higher percentages of S phase cells than vector-alone controls, probably because cell death was efficiently rescued by BCL2 and BCL-x_L. In

contrast to the MycER cells in which BCL-x_L and BCL2 inhibited both cell cycle and cell death, BCL-x_L and BCL2 did not inhibit E2F-induced cell cycle progression, but inhibited E2F-induced apoptosis. These findings suggested that BCL-x_L and BCL2 acted after Myc but before E2F in delaying cell cycle entry.

Cyclin/cdk activities were inhibited in BCL-x_L- and BCL2-expressing cells

Activation of cyclin/cdk complexes occurs downstream of Myc induction, and is key in mediating cell cycle entry. To determine whether BCL-x_L and BCL2 affected the activities of G1 cyclin/cdks, cdk2 and cdk4 complexes were immunoprecipitated from control and BCL-x_L-expressing cells at time points following induction of cell cycle entry and assayed for their ability to phosphorylate GST-Rb. In NIH3T3 cells, both cyclinD/cdk4 and cyclinE/cdk2 kinase activities were significantly downregulated after 48 h of serum starvation (Figure 2), consistent with G0/G1 arrest. Both kinase activities gradually increased after re-addition of serum, beginning at 6 h in pBabe cells. Cdk4 activity reached maximum at 12 h after serum induction, while cdk2 activity was still rising at 15 h. In BCL-x_L-expressing cells, the induction of cyclin/cdk activities was delayed by 3 h, beginning at 9 h after serum addition. BCL-x_L expression did not alter the level of cdk4 protein, which was constant throughout. The total level of cdk2 was also constant; however, there was a difference in the amount of the faster migrating band of cdk2, which is the active form, between BCL-x_L cells and control cells at later time points. In NIH3T3/pBabe cells, the conversion of the cdk2 band from the slower migrating band to the faster active band was observed by Western analysis at 9 h after serum stimulation, corresponding to kinase activation. Conversion to the active cdk2 band was

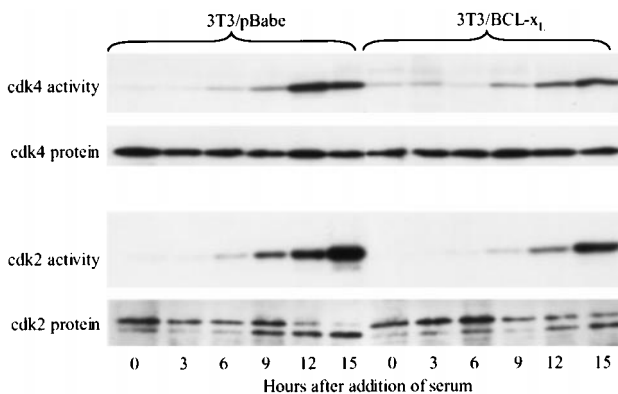
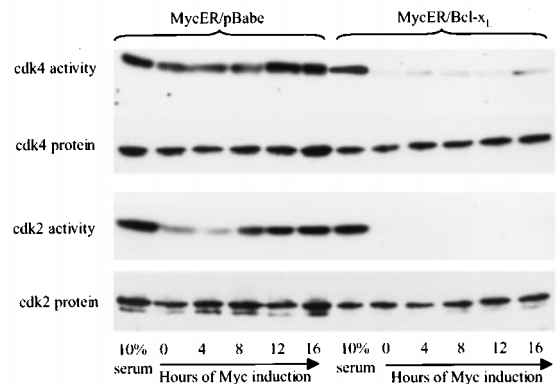


Figure 2 Activation of cdk4 and cdk2 are delayed in NIH3T3 cells expressing BCL-x_L. Cdk4 and cdk2 were immunoprecipitated from NIH3T3 cells expressing BCL-x_L (3T3/BCL-x_L) or pBabe vector (3T3/pBabe) which were serum starved (time 0) or restimulated with 10% BS at the indicated times and assayed for GST-RB kinase activity using [³²P]ATP or immunoblotted for cdk4 or cdk2 protein. The upper band in the cdk2 blot is the inactive form and the lower band is the active form

not observed in BCL-x_L cells until 12 h, consistent with delayed kinase activation. Similar results were obtained with cells expressing BCL2 (data not shown). These findings showed that the delay of serum-induced cell cycle entry by BCL-x_L was accompanied by delayed activation of cdk4 and cdk2.

Next, we asked whether cdk4 and cdk2 activities were also decreased in BCL-x_L or BCL2-expressing cells during Myc-induced cell cycle entry. Following Myc induction in control Rat1 cells, cyclin D/cdk4 activity was present at 4 and 8 h, and reached maximum at 12 h (Figure 3A). Cyclin E/cdk2 activity was similarly induced by 8 h. Induction of cyclin/cdk activities was correlated with cells entering S phase at 4 h and being well into S phase at 12 h. In MycER/BCL-x_L cells, both cyclin D/cdk4 and cyclin E/cdk2 activities were virtually abolished after 48 h of serum starvation. Consistently, only the inactive form of cdk2 protein was detected by Western analysis in MycER/BCL-x_L cells, while the faster migrating active cdk2 was also present in MycER/pBabe cells. It is unclear why the activation of cyclin E/cdk2 in MycER/pBabe cells after Myc induction was not associated with more of a shift to the faster migrating form on Western blots, as seen with the previous experiment (Figure 2) and a later experiment (Figure 6B, cdk2 IP #2).

A. Myc induction



B. Serum induction

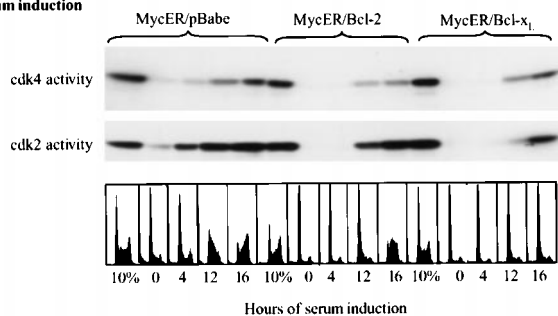


Figure 3 Activation of cdk4 and cdk2 is inhibited in Rat1MycER cells expressing BCL-x_L and BCL2. Cells were serum starved for 48 h and stimulated to re-enter the cell cycle with 4-OHT (A) or 10% serum (B) and assayed at the indicated times for cdk4 and cdk2 kinase activities as in Figure 2, except cdk2 protein was detected by direct Western of cell lysates. Cell cycle profiles are shown below the indicated time points

Differences in antibody specificity may be one possible explanation in that cdk2 protein was detected by a rabbit antibody on Western blotting in Figure 3, while in Figure 2, cdk2 protein was detected by immunoprecipitation with a goat antibody followed by Western blotting with the rabbit antibody. Compared to MycER control cells, BCL-x_L cells achieved a much more complete G₀/G₁ arrest (Figure 1B). In contrast to MycER/pBabe cells, induction of MycER in BCL-x_L cells was not associated with any rise in cdk activities, which remained undetectable at 16 h after 4-OHT treatment (Figure 3A), consistent with the lack of S phase progression (Figure 1B). Similar results were obtained with MycER/BCL2 cells. Thus, the delay in S phase progression in BCL-x_L- and BCL2-expressing cells was correlated with abrogation of Myc-induced cyclin/ckd activation.

To determine whether the dramatic inhibition of cyclin/ckd activities by BCL-x_L was specific to MycER induction or was cell line specific, we stimulated cell cycle entry of starvation-arrested MycER cells with serum (Figure 3B). Cdk4 activation was detectable at 4 h and became readily apparent by 12 h of serum stimulation, and cdk2 activation occurred by 4 h. The majority of cells reached S phase by 12 h after addition of serum. Serum stimulation of MycER/BCL2 or MycER/BCL-x_L cells resulted in delayed cell cycle entry by approximately 4 h. Cdk4 activity was detectable at 12 h but remained lower than in MycER/pBabe cells. Activation of cdk2 in BCL2 and BCL-x_L cells was delayed from 4 to 12 h, and overall kinase activity was reduced, especially in BCL-x_L cells. Therefore, in both Myc-induction and serum-induction, delay of progression to S phase by BCL2 or BCL-x_L was associated with delayed and reduced cyclin D/ckd4 and cyclinE/ckd2 activation. In addition, the effect of BCL-x_L and BCL2 was much more pronounced in Myc-induced than in serum-induced cell cycle entry.

Protein levels of G1 cyclins and cdk4 were unaltered in BCL-x_L cells

Since cdk4 and cdk2 activities are regulated by complex formation with cyclin D and cyclin E, respectively, we examined the induction of cyclin D and cyclin E proteins in BCL-x_L cells compared to controls during serum stimulated cell cycle entry of NIH3T3 cells and Myc stimulated cell cycle entry of Rat1MycER cells. In NIH3T3 control cells, cyclin D1 expression was minimal in serum starvation, but was induced after 6 h of serum stimulation, before entry into S phase (Figure 4A). This is consistent with the requirement of cyclinD/ckd activity prior to progression to S phase. In BCL-x_L expressing cells, cyclin D1 levels at all time points were very similar to control cells, indicating that induction of cyclin D1 was not significantly affected by BCL-x_L expression (Figure 4A). Induction of cyclin D2 was also similar between BCL-x_L expressing and control cells (Figure 4A). Cyclin D3 levels were constant in these cells

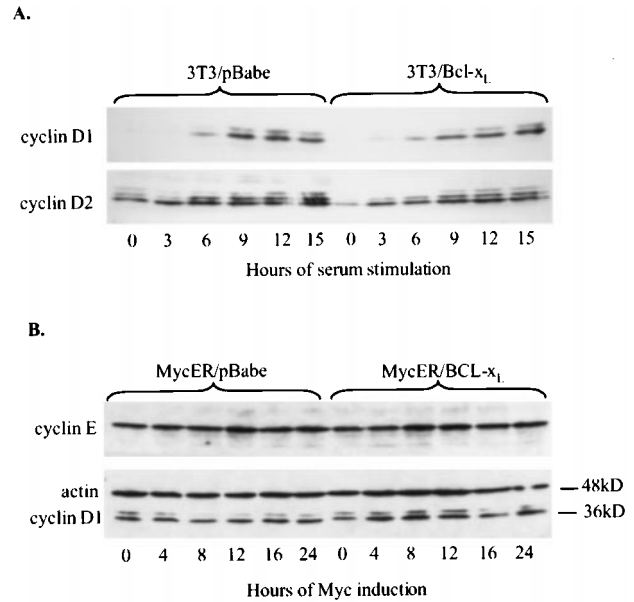


Figure 4 Cyclin D and cyclin E expressions were not altered by BCL-x_L expression. (A) Lysates of NIH3T3 cells expressing BCL-x_L (3T3/BCL-x_L) or vector alone (3T3/pBabe) which were serum starved or stimulated with 10% CS for the indicated times were immunoblotted for cyclin D1 and cyclin D2. (B) Lysates of Rat1-MycER/BCL-x_L or Rat1MycER/pBabe cells which were serum starved and stimulated with 4-OHT for the indicated times were immunoblotted for cyclin D1, cyclin E, and β-actin

throughout the cell cycle (data not shown). We did not detect significant changes in cyclin D1 level during cell cycle progression in Rat1MycER cells. No difference in cyclin D1, D2, or D3 levels was observed between BCL-x_L or BCL2-expressing cells and control MycER cells (Figure 4b and data not shown). Although cyclin E kinase activity rises dramatically during G₁ to S transition, no variations in cyclin E protein levels were detected in control or BCL-x_L-expressing NIH3T3 or Rat1/MycER cells (Figure 4B and data not shown).

p27 protein level was elevated in cells expressing BCL-x_L and BCL2

Cyclin/ckd activities are also regulated by the binding of cdk inhibitors, such as p27 in these cells. In cell cycle arrest, p27 levels are high, and cyclin/ckd activities are inhibited. Cell cycle progression is associated with rapid degradation of p27 and activation of cyclin/ckd complexes. To determine whether cdk2 and cdk4 activities in BCL-x_L cells were inhibited by the increased p27 protein, serum starved NIH3T3 cells expressing BCL-x_L, BCL2, or vector alone were stimulated with 10% FCS and harvested for immunoblot analysis of p27 at 3-h intervals until cells reached S phase (Figure 5A). Higher p27 levels were observed in BCL-x_L cells at the end of serum starvation and at all time points after the addition of serum. As cells entered cycle, p27 levels in BCL-x_L cells decreased as in

control cells; however, the absolute amount of p27 remained higher in BCL-x_L cells. MycER/pBabe and MycER/BCL-x_L or MycER/BCL2 cell lysates were collected at consecutive timepoints after the addition of 4-OHT to serum starved cells. In MycER/pBabe cells, we observed a rise in p27 levels after 48 h of serum starvation, and a gradual decrease after Myc induction, consistent with cell cycle entry. p27 protein levels were significantly elevated in BCL-x_L and BCL2 expressing MycER cells compared to controls at all timepoints examined (Figure 5B,C), similar to the finding in NIH3T3 cells. While the difference in p27 levels was unremarkable between BCL-x_L or BCL2 cells and control cells in asynchronous cultures grown in 10% FCS, p27 accumulated to a much higher level

in BCL-x_L and BCL2 cells arrested in G0/G1 (Figure 5D). This indicated that BCL2 and BCL-x_L affected p27 mainly during cell cycle exit or during quiescence, rather than during proliferation. Other cdk inhibitors, including p21 (Figure 5B) and the INK family member p16 (data not shown), were either not significantly affected by BCL-x_L or BCL2 expression or were not expressed to any significant degree in these Rat1 MycER cells. These data suggested that cyclin/cdk activities in BCL-x_L or BCL2 cells could be inhibited by increased p27, and that upregulation of p27 could be a specific effect of BCL-x_L or BCL2 expression.

Excess p27 saturate cyclin/cdk complexes during Myc induction

Binding of p27 to cyclin/cdk complexes inhibits cdk activity. To determine whether excess p27 in BCL-x_L or BCL2 cells is complexed with cyclin/cdks, thereby inhibiting cdk4 and cdk2 activity and delaying S phase progression, cyclin/cdk complexes were immunoprecipitated and immunoblotted for p27. Immunocomplexes of cdk4 from serum-induced NIH3T3 cells contained significantly higher amounts of p27 in BCL-x_L expressing cells compared to control cells (Figure 6A), suggesting that increased p27 in BCL-x_L cells inhibited cdk4 activation. In arrested control cells at hour 0 and hour 3, cyclin D was not present, and cdk4 immunoprecipitates contained minimal p27, consistent with p27's preferential binding of p27 to cdks which are already complexed with cyclins. In BCL-x_L-expressing cells, p27 was easily detectable in cdk4 immunocomplexes probably because of its abundance. It is likely that more p27 was bound to cdk2. Cdk4 complexes do not associate exclusively with p27 but are also inactivated by other cdk inhibitors such as p21 and INK4 family members, which could be inactivating cdk4 in our NIH3T3 cells.

Myc directly induces cyclin D1 and D2, and p27 is sequestered by cyclin D/cdk4 complexes upon Myc induction, allowing activation of cyclin E/cdk2 and S phase progression (Bouchard *et al.*, 1999; Perez-Roger *et al.*, 1997, 1999). Thus, Myc effectively causes a relocation of p27 from cyclin E/cdk2 complexes to cyclin D/cdk4 complexes. While binding of p27 to cyclin D/cdk4 can inactivate the kinase, a small amount of p27 association is required for cdk4 activity (Cheng *et al.*, 1999). Since p27 levels were high in BCL-x_L cells, and the cyclin/cdk activities were efficiently inhibited, we asked whether the excess p27 was found in the known cyclin/cdk complexes.

Sequential immunoprecipitation-Western analyses were performed to determine whether the excess p27 in BCL-x_L-expressing cells was complexed with cyclin D/cdk4 or cyclin E/cdk2, or was free. Immunoprecipitations to deplete cyclin D complexes followed by immunoprecipitations to deplete cyclin E complexes were performed in MycER/pBabe and MycER/BCL-x_L cell lysates after induction of Myc in serum deprived cultures. To determine in which complexes p27 was located in these cells, the serially immunoprecipitated

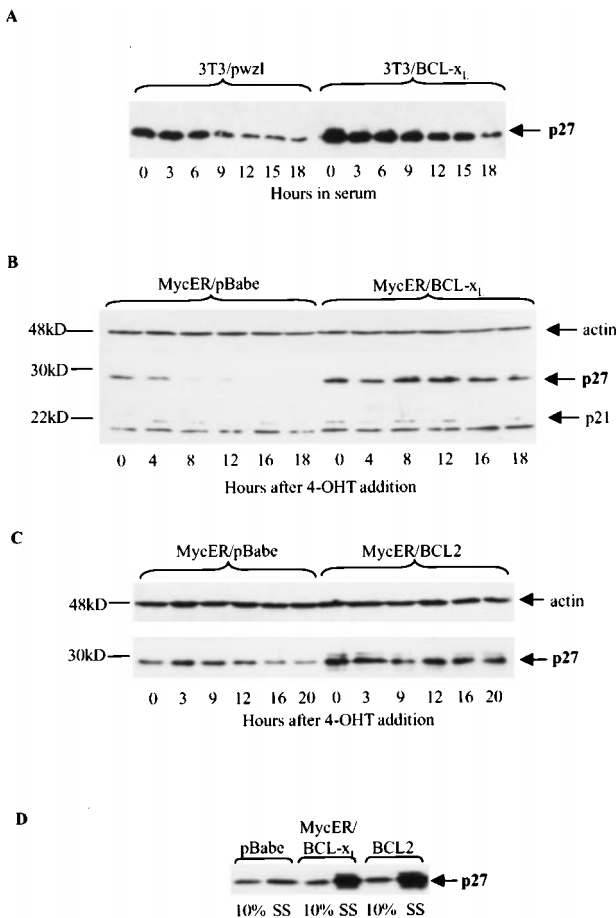


Figure 5 BCL-x_L and BCL2 expressing cells exhibit high p27 levels during serum deprivation and cell cycle re-entry. (A) Lysates of NIH3T3 cells stably expressing BCL-x_L (3T3/BCL-x_L) or retroviral vector alone (3T3/pwz1) cultured in 10% CS, 0.75% CS for 2 days, or re-stimulated with 10% CS were collected at indicated times and immunoblotted with p27 antibody. (B,C) Lysates of Rat1MycER cells retrovirally infected with pBabeBCL-x_L, pBabeBCL2, or pBabe vector were collected after serum starvation and at indicated times after the addition of 4-OHT and immunoblotted for p27, p21, and β-actin. (D) p27 levels in MycER cells expressing BCL-x_L, BCL2, or pBabe vector cultured in 10% FCS (10%) and after 48 h of serum starvation (SS) were compared by Western blotting of total lysates

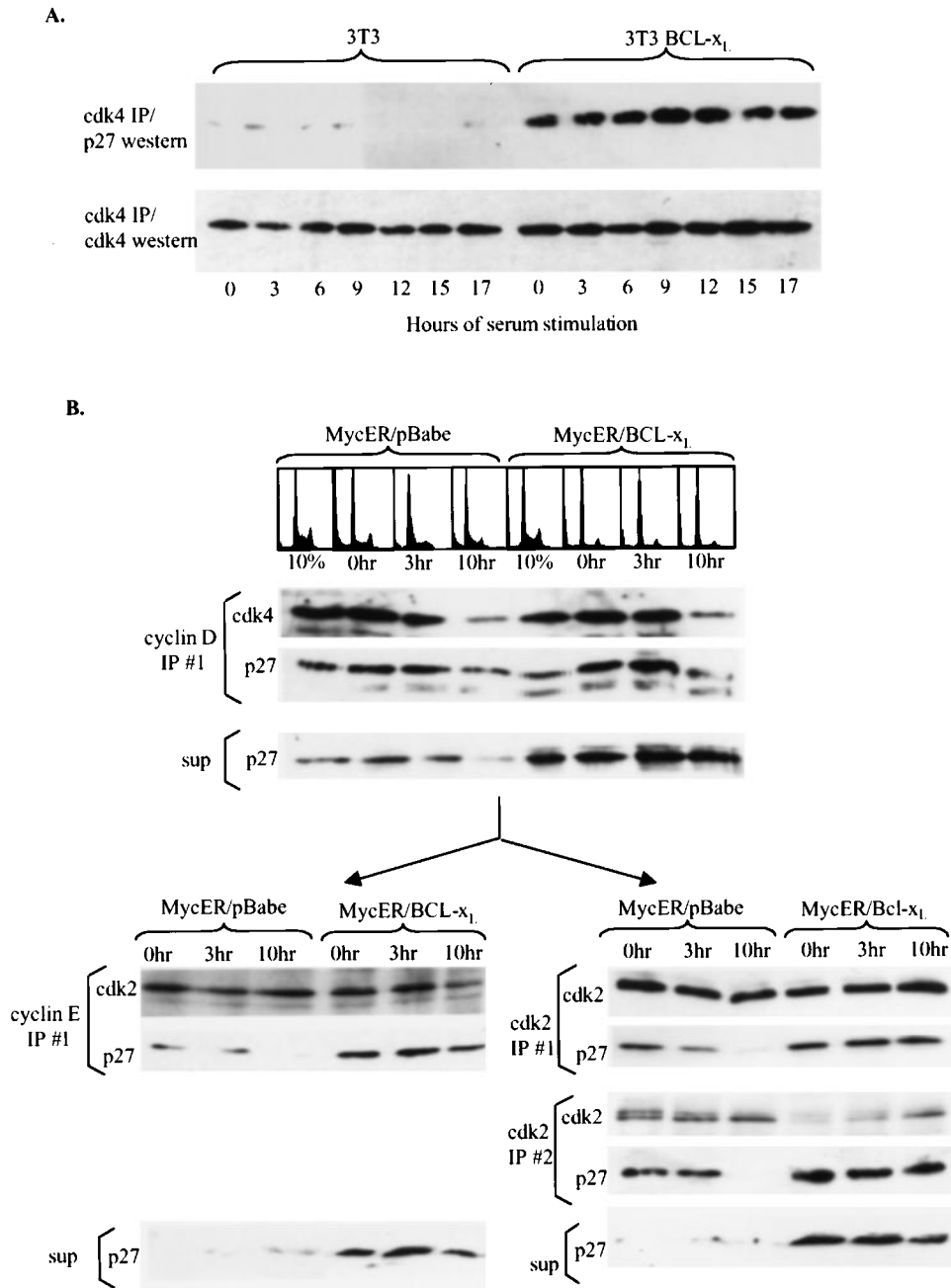


Figure 6 Cdk4 and cdk2 complexes from BCL-x_L expressing cells contain excess p27, and p27 is not sequestered away from cdk2 complexes in Myc-induced cell cycle entry. **(A)** Cdk4 was immunoprecipitated (IP) from serum starved or serum stimulated NIH3T3/BCL-x_L or NIH3T3/pBabe cells at the indicated times and Western blotted for cdk4 or p27. **(B)** Lysates of MycER/BCL-x_L or MycER/pBabe collected before serum starvation and at 0, 3, and 10 h after serum starvation + 4-OHT treatment were subjected to IP with a mixture of cyclin D1, D2, and D3 antibodies and immunoblotted for cdk4 and p27 (cyclin D IP#1). The same lysate was subjected to a second round of IP with cyclin D1, D2, and D3 antibodies, which did not yield detectable cyclin/cdk4 complexes and is not shown. An aliquot of the supernatant after two rounds of cyclin D IPs was immunoblotted for p27 (sup). The rest of the supernatant was divided into two parts. One part was subjected to two sequential cyclin E IPs and immunoblotted for cdk2 and p27 (cyclin E IP #1). The second cyclin E IP was clean of cyclin E/cdk2 complexes and is not shown. The lysate remaining after the cyclin D and cyclin E immunodepletions was immunoblotted for p27 (sup). The second part of the supernatant after cyclin D IPs was subjected to cdk2 IP with anti-cdk2 twice and immunoblotted for cdk2 and p27 (cdk2 IP#1, cdk2 IP#2). The supernatant after cyclin D and cdk2 immunodepletions was immunoblotted for p27 (sup). Cell cycle profiles of the cultures at the time of collection are shown

complexes and the supernatant remaining after all the immunodepletions were Western blotted for p27 (Figure 6B). Cell extracts from 0, 3, and 10 h after 4-OHT induction were depleted twice by a mixture of

cyclin D1, D2, and D3 antibodies. The majority of cdk4 was found in the first round of cyclin D immunoprecipitation, and p27 was detected at similar levels in the cyclin D/cdk4 complexes in control and in

BCL-x_L expressing cells (Figure 6B, top panel, cyclin D IP #1). Minimal cdk4 was found in the second round of cyclin D immunoprecipitation, and no p27 was detectable (not shown), indicating that cyclin D complexes had been efficiently depleted from the lysate. Interestingly, p27 was significantly more abundant in the depleted extracts of BCL-x_L-expressing cells at all three time points (Figure 6B, top panel, sup), indicating that the excess p27 was not bound in the cyclin D complexes, but in some other complexes instead.

The cyclin D-depleted extracts were then divided into two equal parts. One part was depleted of cyclin E complexes by two serial immunoprecipitations, and the other part was depleted twice with cdk2 immunoprecipitations. In contrast to cyclin D complexes, more p27 was found in the cyclin E complexes from BCL-x_L expressing cells before (0 h) and after Myc induction (3 and 10 h). While p27 was no longer present in the cyclin E complex of control cells by 10 h after Myc induction when cells were well into S phase, p27 was still present in the cyclin E complex of BCL-x_L cells, presumably inhibiting cyclin E/ckd2 activity and delaying cell cycle progression (Figure 6B, lower left panel, cyclin E IP#1). No significant cdk2 and no p27 was detected in the second round of cyclin E immunoprecipitation (not shown), indicating efficient depletion of cyclin E complexes by the first round of immunoprecipitation. No p27 was present in the cyclin D- and cyclin E-depleted extract of MycER/pBabe cells at 0 and 3 h, indicating that all the p27 was bound to either the cyclin D or cyclin E complexes. A small amount of p27 was detected in the depleted extracts at 10 h in control cells, presumably released from cyclin E prior to cells entering S phase. In contrast, significant p27 remained in the cyclin D and cyclin E depleted extracts from BCL-x_L cells at all three time points (Figure 6B, lower left panel, sup). Thus, excess p27 saturated cyclin D and cyclin E complexes in BCL-x_L cells, inhibiting progression to S phase, and more p27 still remained unbound.

Cdk2 was also immunoprecipitated twice from the cyclin D-depleted extracts (Figure 6B, lower right panel). Similar to the cyclin E immunoprecipitations, p27 was present in the cdk2 complexes at 0 and 3 h in control cells, but absent from cdk2 complexes at 10 h when cells were well into S phase. However, in BCL-x_L cells, more p27 was complexed with cdk2 at all three time points, and still more unbound p27 remained in the supernatant after two rounds of immunoprecipitations to deplete cdk2 (Figure 6B, lower right panel, sup). These immunodepletion experiments showed that in BCL-x_L-expressing cells, excess p27 persisted in cyclin E/ckd2 complexes after Myc induction, such that cdk2 was not activated and cell cycle progression was inhibited.

BCL2 and BCL-x_L require p27 to delay cell cycle entry

To determine whether elevated p27 level was required for BCL2 or BCL-x_L to delay cell cycle entry, we asked whether BCL2 or BCL-x_L could delay entry into S

phase in cells lacking p27. Mouse embryo fibroblast lines from p27^{+/+} and p27^{-/-} littermates were retrovirally infected with pBabe, pBabeBCL2, or pBabeBCL-x_L, serum deprived, and released into cell cycle by serum addition. Progression into S phase was measured by BrdU incorporation (Figure 7). In wildtype MEFs, BCL2 or BCL-x_L expression delayed BrdU incorporation by approximately 4 h, similar to NIH3T3 cells. In contrast, there was no difference in the rate of BrdU incorporation between p27^{-/-} MEFs expressing BCL2, BCL-x_L, or vector alone. This result indicated that the ability of BCL2 or BCL-x_L to delay cell cycle entry required the presence of p27, suggesting that increased p27 was a specific effect of BCL2 or BCL-x_L expression.

Discussion

We have temporally mapped the cell cycle activity of BCL2 and BCL-x_L by using cell lines with inducible alleles of genes that regulate the G0-S transition. BCL2 and BCL-x_L very effectively blocked cell cycle entry induced by MycER, but had no effect on cell cycle progression induced by a tetracycline regulated E2F-1 allele. This placed the activity of BCL2 and BCL-x_L between Myc and E2F-1. Induction of Myc is an early event in cell cycle entry, occurring within 2 h after serum stimulation (Persson *et al.*, 1985; Rabbitts *et al.*, 1985). Inhibition of Myc-induced cell cycle entry indicated that BCL2 and BCL-x_L interfered with events downstream of the Myc pathway, rather than completely preventing the initiation of cell cycle entry. However, BCL2 or BCL-x_L did not delay cell cycle progression induced by E2F-1, which is believed to function at the G1-S transition. Cyclin D upregulation occurs after Myc induction in cell cycle entry. Further timing of BCL2 and BCL-x_L activity using inducible cyclin D cells were inconclusive (data not shown), because cell cycle acceleration by cyclin D also requires

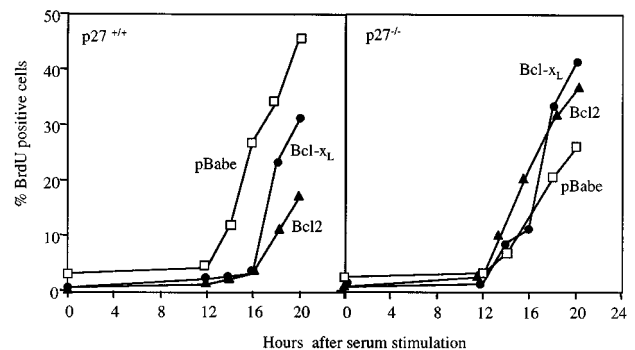


Figure 7 BCL-x_L and BCL2 delay cell cycle entry in p27^{+/+}, but not p27^{-/-}, MEFs. p27^{+/+} and p27^{-/-} MEFs infected with pBabepuro containing BCL-x_L, BCL2, or empty vector were cultured in 0.1% FCS for 2 days, then stimulated with 10% FCS. BrdU incorporation was measured at the indicated times, and per cent of BrdU positive cells was plotted against time after serum addition. Results shown are representative of duplicate experiments

the presence of serum (Resnitzky *et al.*, 1994; Resnitzky and Reed, 1995). However, Western blots demonstrating normal induction of cyclin D1 protein in BCL2 or BCL-x_L cells (Figure 4) suggested that BCL2 and BCL-x_L acted after, or in parallel to, cyclin induction, placing the activity of BCL2 and BCL-x_L between cyclin D and E2F-1 induction.

We consistently observed elevation of p27 protein during cell cycle arrest and inhibition of cyclin/cdk activities in fibroblasts expressing BCL2 and BCL-x_L. BCL2 and BCL-x_L cells accumulated enough p27 to saturate cyclin/cdk complexes, inhibiting their activity, and had excess p27 which may affect other cell cycle pathways. The effect of BCL2 and BCL-x_L on p27 occurred specifically in cells undergoing arrest, because cycling BCL2 and BCL-x_L cells had normal or near normal amounts of p27. Inability of BCL2 or BCL-x_L to delay cell cycle in p27^{-/-} MEFs suggests that the increase in p27 was causal to the cell cycle activity of BCL2 and BCL-x_L. In addition, cyclin D1 induction in BCL2 or BCL-x_L cells was not impaired despite delayed cell cycle progression. Our data suggest that BCL2 and BCL-x_L affect the activities of G1 cyclin/ckds post-translationally through p27, which is required for the cell cycle delay function of BCL2 and BCL-x_L. How BCL-x_L and BCL2 expression causes elevation of p27 in arrested cells has yet to be addressed. p27^{-/-} MEFs arrested in the absence of serum and entered cycle at the same time as wildtype MEFs, obviously using pathways independent of p27, and BCL2 had no effect on these pathways. Interestingly, preliminary observations suggest that the anti-apoptotic activity of BCL2 and BCL-x_L does not require p27 (data not shown), consistent with the anti-apoptosis and cell cycle delay functions of BCL2 and BCL-x_L being separable.

The cell cycle delay activity of BCL2 and BCL-x_L was more profound in 4-OHT induced MycER cells than in serum induced cell cycle entry. Activation of cyclin E/cdk2 is important in Myc-induced G1-S transition. Myc activates cyclin E/cdk2 by interfering with the binding of the cdk inhibitor p27 to cyclin E/cdk2 complexes. Myc induces Cull1, a component of the SCF^{SKP2} complex, leading to degradation of p27 (O'Hagan *et al.*, 2000). Myc also represses p27 transcription (Yang *et al.*, 2001). In addition, immunodepletion experiments revealed that Myc induces cyclin D1 and cyclin D2 proteins, which sequester p27, resulting in activation of cyclin E/cdk2 (Perez-Roger *et al.*, 1999; Bouchard *et al.*, 1999). Using a similar immunodepletion approach, we found that high levels of p27 remained in the cyclin E/cdk2 complexes in BCL2 and BCL-x_L-expressing cells after Myc induction. Cyclin E/cdk2 remained inactive and cell cycle progression was delayed. The amount of cyclin D/cdk4 complexes and the amount of p27 detected in these complexes from MycER/pBabe cells and MycER/BCL-x_L cells were similar, consistent with our finding that BCL2 or BCL-x_L did not alter the induction of cyclin D protein. Nevertheless, BCL2 and BCL-x_L inhibited Myc-induced activation of cdk4 and cdk2. The

inhibition was quite stringent in MycER cells, as we did not detect a rise in cyclin/cdk activities even at later time points when BCL2 or BCL-x_L cells entered S phase. It is possible that the BCL2 and BCL-x_L cells enter S phase by mechanisms independent of cyclin E/cdk2. For example, Myc induces transcription of E2F-1, E2F-2, and E2F-3 genes, and the Myc/E2F pathway is essential for Myc-induced S phase, as well as Myc-induced apoptosis (Adams *et al.*, 2000; Leone *et al.*, 2001; Sears *et al.*, 1997). In serum-induced cell cycle entry, BCL2 and BCL-x_L delayed, but did not abolish, cyclin/cdk activation, which occurred approximately 3–4 h later than control cells. In NIH3T3 cells, more p27 was found in cyclin D/cdk4 complexes in the BCL-x_L cells than in control cells, whereas in induced MycER cells, cyclin D complexes may already be maximally saturated with p27, so that BCL-x_L expression could not further increase p27 association. Addition of serum to arrested cells stimulates the Myc pathway, which can be inhibited by BCL2 or BCL-x_L, as well as pathways besides Myc which are presumably unaffected by BCL2 or BCL-x_L. The end result is a shorter delay in activation of cyclin/ckds and progression to S phase by BCL2 or BCL-x_L in serum stimulated fibroblasts.

Previous reports showed that BCL2 did not affect MycER-induced proliferation as assayed by first cell divisions using time-lapsed cinemicroscopy, but BCL2 effectively inhibited apoptosis induced by MycER in serum-deprived cultures (Fanidi *et al.*, 1992). The ability of BCL2 to inhibit the apoptotic activity of Myc without affecting its proliferative function explained the mechanism for the cooperativity between BCL2 and Myc in tumorigenesis (Hueber and Evan, 1998). Here, we found that Myc-induced S phase entry was almost completely blocked by BCL2 or BCL-x_L, and the doubling rate of BCL2 and BCL-x_L cells was slightly prolonged in asynchronous cultures grown in 10%FCS (data not shown). Our experiments measured S phase entry by BrdU incorporation and cell cycle profiles based on DNA content, while the time-lapsed cinemicroscopy experiments only registered cells which had successfully completed mitosis, and all cells which underwent apoptosis were excluded from analysis even though they might have entered S phase before dying. Myc-induced apoptosis occurs in both G1 and G2 (Hengstschlager *et al.*, 1999). We observed exuberant S phase progression in the first few hours of Myc induction in control cells, but apoptosis became significant before 24 h, thus most of the induced cells do not survive through G2/M and would not be scored by the cinemicroscopy experiments. Consistent with our results, there was a difference between BCL2 and control MycER cells in the early time points on the graph measuring first divisions (Fanidi *et al.*, 1992). Thus, our data demonstrate that BCL2 and BCL-x_L delay Myc-induced G0/G1 to S progression, while previous data found BCL2 did not affect ultimate proliferation induced by Myc.

Recently, Myc was reported to cause transcriptional downregulation of BCL2 and BCL-x_L in IL-3

dependent cells (Eischen *et al.*, 2001a) and bone marrow cells (Eischen *et al.*, 2001b), respectively. Transcriptional repression occurred quickly in these cells, but the protein levels did not decrease significantly until 20–24 h after Myc induction. We also observed somewhat lower endogenous BCL-x_L and BCL2 protein levels in fibroblasts after MycER induction (data not shown), however, the decreases occurred long after cells have already entered S phase, and therefore, are not likely to be the explanation for present experimental findings.

Results presented here suggest a model in which BCL2 and BCL-x_L interfere with Myc activity in cell cycle by upregulating p27 protein level. Our finding that BCL2 and BCL-x_L cannot delay cell cycle in MEFs in the absence of p27 is consistent with a previous report that BCL2 did not delay activation-induced cell cycle entry in *p27*^{-/-} T cells (Vairo *et al.*, 2000). In addition, BCL2 was shown to function through the pRB relative p130, which negatively regulates progression to S phase (Lind *et al.*, 1999; Vairo *et al.*, 2000). Thus, BCL2 can delay cell cycle by upregulation of p130 and upregulation of p27, two proteins that affect overlapping pathways. Investigations presented here focused on the upregulation of p27 in BCL2 and BCL-x_L expressing cells. Our data suggest that BCL-x_L and BCL2 interfere with the ability of Myc to downregulate p27 and activate cyclin/cdks, and point to downstream events of Myc as targets of BCL2 and BCL-x_L.

Materials and methods

Cell culture

Fibroblasts were maintained in Dulbecco's Modified Eagle Medium (DMEM) supplemented with 10% fetal calf serum (FCS) or calf serum (CS), 2 mM L-glutamine and 100 u penicillin/streptomycin per ml (BioWhittaker). In Rat1 MycER cells (gift of Dr Gerard Evan), Myc expression was induced by the addition of 200 μM 4-hydroxytamoxifen (4-OHT) to the media at 200 nM. Rat2FBX40 cells (gift of Dr Wen-Hwa Lee) (Shan and Lee, 1994) were maintained in DMEM supplemented with 10% FCS, and tetracycline (1 μg/ml). Primary *p27*^{-/-} embryonic fibroblasts were obtained from *p27*^{+/-} matings harvested at E13.5 (kindly provided by Dr Carlos Arteaga, Vanderbilt Ingram Cancer Center), and passed through a 3T3 protocol. BCL2 and BCL-x_L were introduced into these cells via retroviral infection. pBabepuro constructs containing full length BCL2 (human) or BCL-x_L (mouse) were transfected using calcium phosphate into BOSC cells. Two days later, viral supernatant was collected, filtered, and used to infect the fibroblasts at 2-h intervals for four times. Cells were selected in media containing puromycin (4 μg/ml).

Cell cycle analysis

To obtain cell cycle profiles, cells were seeded into 6-well dishes. The next day, cells were washed three times with phosphate-buffered saline (PBS) and incubated in media containing 0.01% FCS (Rat2FBX40), 0.05% FCS (Rat1MycER), or 0.75% CS (NIH3T3). After 48 h of serum starvation, the cells were stimulated by the re-addition of media containing 10% serum. At designated times, cells were trypsinized, centrifuged, and resuspended in Krishan's

reagent (0.1 mg/ml propidium iodide, 0.02 mg/ml RNase A, 0.3% NP-40, and 0.1% Na Citrate). The DNA content of 10 000 cells/sample was measured on a FACSCalibur (Becton-Dickinson). For BrdU pulse labeling/propidium iodide experiments, cells were seeded onto 100 mm dishes. At indicated times, cells were pulsed for 30 min with 20 μM BrdU (Sigma) trypsinized, and fixed by drop-wise addition of cold 70% ethanol. 4N HCl was added to the fixed cells, neutralized by 0.1 M borax, and washed with PBS containing 0.5% BSA. The cells were then incubated with anti-BrdU antibody (Becton-Dickinson), followed by incubation with FITC-conjugated anti-mouse secondary antibody (Sigma). All antibodies were diluted in PBS containing 0.5% BSA and 0.5% Tween-20. Finally, cells were resuspended in PBS containing 50 μg/ml propidium iodide and 20 μg/ml RNase A and analysed on the FACSCalibur. All serum starvation and release data were analyzed using Cell Quest and Modfit software programs (Becton-Dickinson).

Western blots and antibodies

Cells were harvested, washed with PBS and lysed in RIPA buffer. Protein concentrations were determined using Bradford reagent (Bio-Rad). After separating the samples (100 μg per lane) on a 12.5% SDS-PAGE, the proteins were transferred to PVDF membrane (Bio-Rad), and blocked in PBS-Tween containing 5% milk. Antibodies were diluted in PBS-Tween and included: Bcl-2 (6C8, Pharmingen); Bcl-x (H-5), CDK2 (M2, goat for IP or rabbit for Western), CDK4 (C22), Cyclin D1 (sc-246 for Western, sc-450 for IP), Cyclin E (M20) (Santa Cruz); p27 (Transduction Labs); Cyclin D1 (DCS-6), Cyclin D2 (DCS 5.2), Cyclin D3 (DCS 28.1) (Neomarkers). HRP-conjugated secondary antibodies were purchased from Jackson Immunoresearch. Proteins were visualized using enhanced chemiluminescence.

Immunoprecipitations and kinase assays

Cells were harvested, washed with PBS and incubated at 4°C in lysis buffer (50 mM Tris pH 7.4, 150 mM NaCl, 4 mM EDTA, 0.1% NP-40, 0.1% Triton X-100, 50 mM NaF, 0.1 mM NaV, and protease inhibitors, phenylmethylsulfonyl fluoride (50 μg/ml) (Sigma), antipain (10 μg/ml), pepstatin A (10 μg/ml), leupeptin (10 μg/ml), chymostatin (10 μg/ml) and 4-(2-amino-ethyl)-benzenesulfonyl fluoride (200 μg/ml) (Calbiochem-Novabiochem Corp)). Total cellular protein was assayed using Bradford reagent (Bio-Rad) and 300 μg protein was used for each sample. Samples were pre-cleared for 45 min prior to the addition of antibody (CDK2 (sc-163), CDK4 (sc-260)), Cyclin D1 (sc-246), cyclin D2 (DCS 5.2), cyclin D3 (DCS 28.1)). After 2 h of antibody incubation, protein A or G sepharose beads were added to the protein-antibody mixture and allowed to incubate for 1 h. For kinase assays, immunoprecipitates were washed twice with kinase lysis buffer (without inhibitors) and twice with kinase assay buffer (100 mM Tris (pH 7.4), 20 mM MgCl₂, 2 mM DTT) prior to the addition of cold ATP (15 nM) and 5 mg GST-RB (aa 792–928) (Meyerson and Harlow, 1994) for 10 min. Next, 10 μCi of [³²P]ATP was added and the reaction was allowed to proceed for 10 min at 30°C before being stopped with 2× Laemli buffer. Kinase assays and immunoprecipitations were resolved on a 12.5% SDS-PAGE gel, transferred to PVDF membrane, which was quantitated on an Instant Imager (Packard Instruments) prior to autoradiography. Proteins captured by the immunoprecipitations were visualized by immunoblotting.

Acknowledgments

We thank Drs Carlos Arteaga and Richard Pestell for providing p27 heterozygous matings and p27^{-/-} MEFs. We thank Drs Scott Hiebert and Stephen Hann for critical reading of the manuscript. We are grateful to Drs Stephen Hann and Chi-Wu Chiang for continuous scientific input

References

- Adams MR, Sears R, Nuckolls F, Leone G and Nevins JR. (2000). *Mol. Cell Biol.*, **20**, 3633–3639.
- Bouchard C, Thieke K, Maier A, Saffrich R, Hanley-Hyde J, Ansorge W, Reed S, Sicinski P, Bartek J and Eilers M. (1999). *EMBO J.*, **18**, 5321–5333.
- Brady HJ, Gil-Gomez G, Kirberg J and Berns AJ. (1996). *EMBO J.*, **15**, 6991–7001.
- Chattopadhyay A, Chiang CW and Yang E. (2001). *Oncogene*, **20**, 4507–4518.
- Cheng M, Olivier P, Diehl JA, Fero M, Roussel MF, Roberts JM and Sherr CJ. (1999). *EMBO J.*, **18**, 1571–1583.
- Cory S, Vaux DL, Strasser A, Harris AW and Adams JM. (1999). *Cancer Res.*, **59**, 1685s–1692s.
- Dijkers PF, Medema RH, Pals C, Banerji L, Thomas NS, Lam EW, Burgering BM, Raaijmakers JA, Lammers JW, Koenderman L and Coffey PJ. (2000). *Mol. Cell Biol.*, **20**, 9138–9148.
- Eilers M, Schirm S and Bishop JM. (1991). *EMBO J.*, **10**, 133–141.
- Eischen CM, Packham G, Nip J, Fee BE, Hiebert SW, Zambetti GP and Cleveland JL. (2001a). *Oncogene*, **20**, 6983–6993.
- Eischen CM, Woo D, Roussel MF and Cleveland JL. (2001b). *Mol. Cell Biol.*, **21**, 5063–5070.
- Evan GI, Wyllie AH, Gilbert CS, Littlewood TD, Land H, Brooks M, Waters CM, Penn LZ and Hancock DC. (1992). *Cell*, **69**, 119–128.
- Fanidi A, Harrington EA and Evan GI. (1992). *Nature*, **359**, 554–556.
- Hengstschlager M, Holz G and Hengstschlager-Ottner E. (1999). *Oncogene*, **18**, 843–848.
- Huang DC, O'Reilly LA, Strasser A and Cory S. (1997). *EMBO J.*, **16**, 4628–4638.
- Hueber AO and Evan GI. (1998). *Trends Genet.*, **14**, 364–367.
- Johnson DG, Schwarz JK, Cress WD and Nevins JR. (1993). *Nature*, **365**, 349–352.
- Kaczmarek L, Hyland JK, Watt R, Rosenberg M and Baserga R. (1985). *Science*, **228**, 1313–1315.
- Leone G, Sears R, Huang E, Rempel R, Nuckolls F, Park CH, Giangrande P, Wu L, Saavedra HI, Field SJ, Thompson MA, Yang H, Fujiwara Y, Greenberg ME, Orkin S, Smith C and Nevins JR. (2001). *Mol. Cell*, **8**, 105–113.
- Lind EF, Wayne J, Wang QZ, Staeva T, Stolzer A and Petrie HT. (1999). *J. Immunol.*, **162**, 5374–5379.
- Linette GP, Li Y, Roth K and Korsmeyer SJ. (1996). *Proc. Natl. Acad. Sci. USA*, **93**, 9545–9552.
- Marin MC, Hsu B, Stephens LC, Brisbay S and McDonnell TJ. (1995). *Exp. Cell Res.*, **217**, 240–247.
- Mazel S, Burtrum D and Petrie HT. (1996). *J. Exp. Med.*, **183**, 2219–2226.
- Medema RH, Kops GJ, Bos JL and Burgering BM. (2000). *Nature*, **404**, 782–787.
- Meyerson M and Harlow E. (1994). *Mol. Cell Biol.*, **14**, 2077–2086.
- O'Hagan RC, Ohh M, David G, de Alboran IM, Alt FW, Kaelin Jr WG and DePinho RA. (2000). *Genes Dev.*, **14**, 2185–2191.
- O'Reilly LA, Huang DC and Strasser A. (1996). *EMBO J.*, **15**, 6979–6990.
- Obaya AJ, Mateyak MK and Sedivy JM. (1999). *Oncogene*, **18**, 2934–2941.
- Perez-Roger I, Kim SH, Griffiths B, Sewing A and Land H. (1999). *EMBO J.*, **18**, 5310–5320.
- Perez-Roger I, Solomon DL, Sewing A and Land H. (1997). *Oncogene*, **14**, 2373–2381.
- Persson H, Gray HE and Godeau F. (1985). *Mol. Cell Biol.*, **5**, 2903–2912.
- Philipp-Staheli J, Payne SR and Kemp CJ. (2001). *Exp. Cell Res.*, **264**, 148–168.
- Rabbits PH, Watson JV, Lamond A, Forster A, Stinson MA, Evan G, Fischer W, Atherton E, Sheppard R and Rabbits TH. (1985). *EMBO J.*, **4**, 2009–2015.
- Resnitzky D, Gossen M, Bujard H and Reed SI. (1994). *Mol. Cell Biol.*, **14**, 1669–1679.
- Resnitzky D and Reed SI. (1995). *Mol. Cell Biol.*, **15**, 3463–3469.
- Sears R, Ohtani K and Nevins JR. (1997). *Mol. Cell Biol.*, **17**, 5227–5235.
- Shan B and Lee WH. (1994). *Mol. Cell Biol.*, **14**, 8166–8173.
- Tomoda K, Kubota Y, Arata Y, Mori S, Maeda M, Tanaka T, Yoshida M, Yoneda-Kato N and Kato Jy J. (2001). *J. Biol. Chem.*, **9**, 9.
- Tomoda K, Kubota Y and Kato J. (1999). *Nature*, **398**, 160–165.
- Vairo G, Innes KM and Adams JM. (1996). *Oncogene*, **13**, 1511–1519.
- Vairo G, Soos TJ, Upton TM, Zalvide J, DeCaprio JA, Ewen ME, Koff A and Adams JM. (2000). *Mol. Cell Biol.*, **20**, 4745–4753.
- Wu X and Levine AJ. (1994). *Proc. Natl. Acad. Sci. USA*, **91**, 3602–3606.
- Yang W, Shen J, Wu M, Arsura M, FitzGerald M, Suldan Z, Kim DW, Hofmann CS, Pianetti S, Romieu-Mourez R, Freedman LP and Sonenshein GE. (2001). *Oncogene*, **20**, 1688–1702.